

Chapter V

Ni(II) Adsorption onto TPVSP and TBVSP

The results related to confiscate Ni(II) using TPVSP and TBVSP from the aqueous matrices and industrial seepages are presented in this chapter.

5.1 Surface Characterization studies

SEM images of TPVSP/ TBVSP along with the Ni(II) loaded counterparts are presented in figures 5.1 (a, b) and 5.2 (a, b). A decline in the smooth and homogeneous surface appearances of TPVSP and TBVSP are observed in 'b' figures, which might be due to the adherence of Ni(II) ions, onto the porous materials possessing suitable binding sites. The EDAX spectra of the precursors and Ni(II) laden materials are illustrated in figures 5.3 (a, b) & 5.4 (a, b) respectively. Prominent peaks in the range of 7- 8 keV indicate that Ni(II) sorption had occurred.

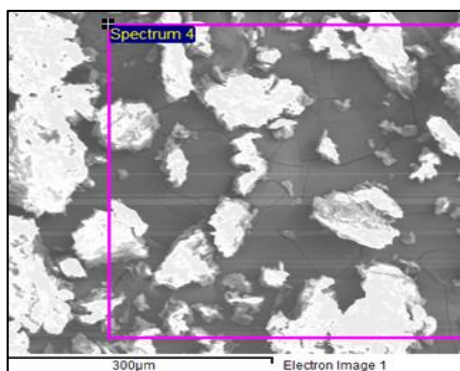


Figure 5.1 (a) SEM -Unloaded TPVSP

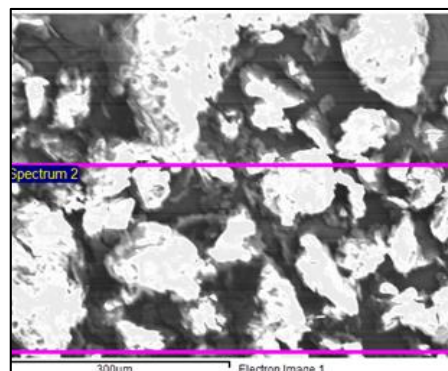


Figure 5.1 (b) SEM -Ni(II)- TPVSP

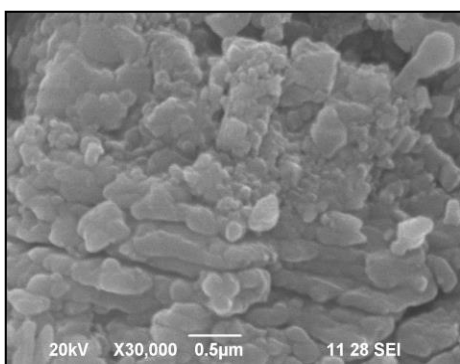


Figure 5.2 (a) SEM -Unloaded TBVSP

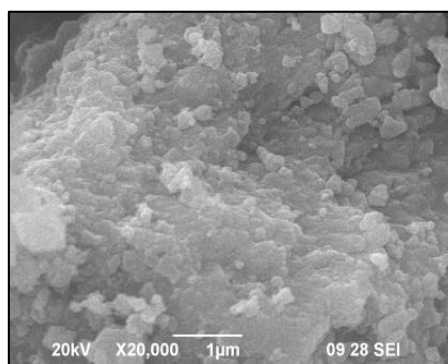


Figure 5.2 (b) SEM -Ni(II) -TBVSP

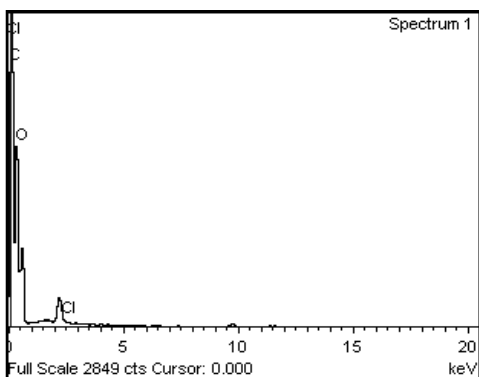


Figure 5.3 (a) EDAX-Unloaded TPVSP

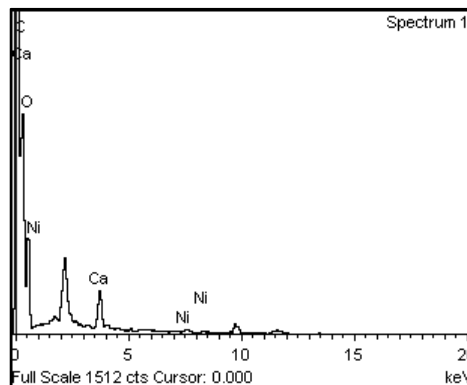


Figure 5.3 (b) EDAX-Ni(II) -TPVSP

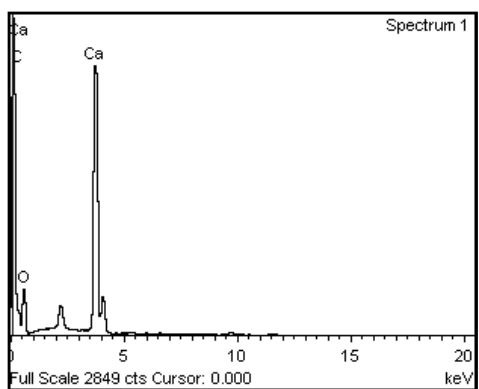


Figure 5.4 (a) EDAX-Unloaded TBVSP

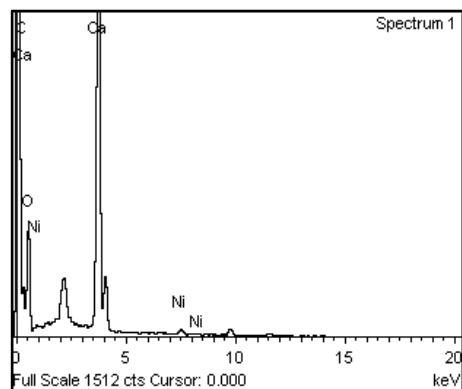
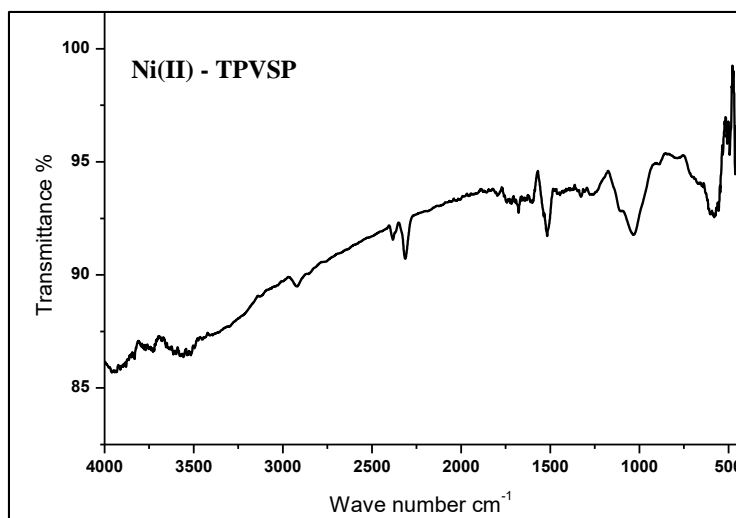


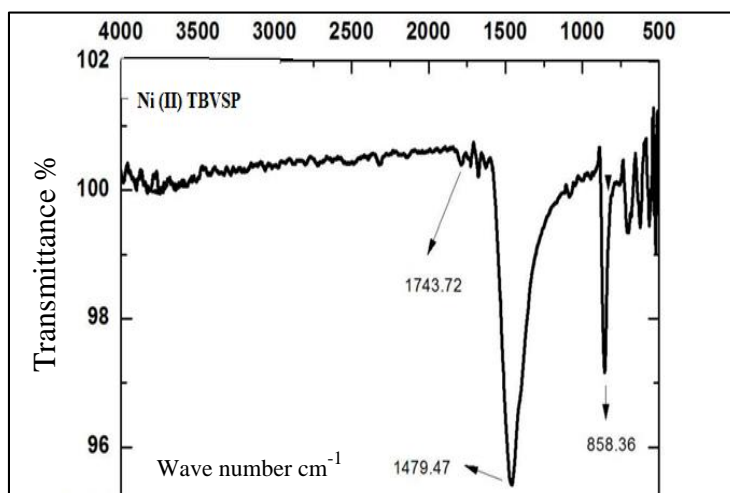
Figure 5.4 (b) EDAX-Ni(II) -TBVSP

5.2 FT-IR Spectral Studies

FTIR spectra of unloaded and Ni(II) loaded TPVSP and TBVSP are shown in figures 5.5 (a and b), with obtained peak values corresponding to the respective functional groups (amino, carboxylic, hydroxyl and carbonyl groups). Inclines and declines in the intensities of the peaks as perceived from these figures, indicate at appropriate shifts had occurred due to Ni(II) uptake by the sorbents, similar to Pb(II) removal.



5.5 (a) FT-IR Spectra Ni(II)- TPVSP



5.5 (b) FT-IR Spectra Ni(II) -TBVSP

5.3 Batch Equilibration Studies

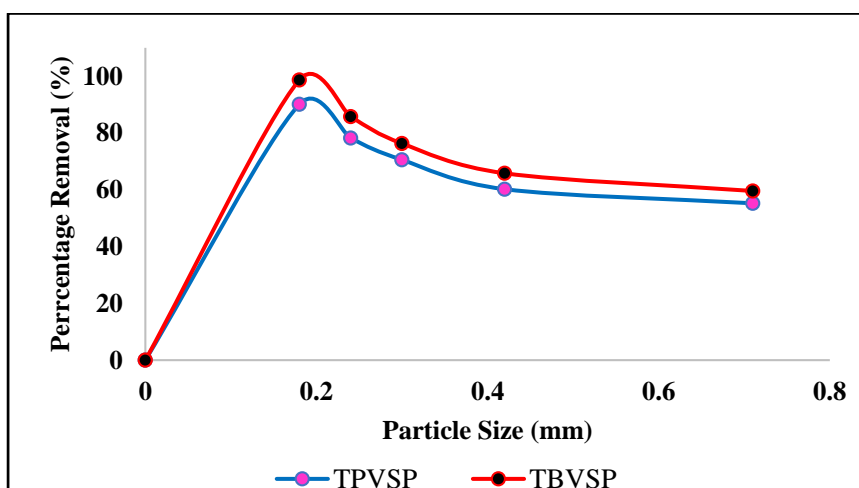
5.3.1 Effect of Particle Size

Table 5.1 registers maximum Ni(II) sorption at smaller particle size (0.18 mm), for both the sorbent materials. This could be reasoned as greater surface area for smaller particle size which in turn increase the available active sites, promoting better removal¹. Also, better sorption performance of TBVSP than TPVSP is obvious from figure 5.6 at 0.18 mm particle size. Therefore, 0.18 mm had been fixed as the optimum particle size for the discussions ahead.

Table 5.1 Effect of Particle Size

Particle Size (mm)	Percentage Removal (%)	
	TPVSP	TBVSP
0.18	90.1	98.7
0.24	78.2	85.8
0.30	70.5	76.3
0.42	60.2	65.8
0.71	55.2	59.6

Adsorbent dose - **100 mg.**, Metal ion concentration- **25 mg/L.**,
Agitation time:**10 mins** Temperature: **303K**

**Figure 5.6 Effect of Particle Size (mm)**

5.3.2 Effect of Initial Concentration and Contact time

Table 5.2 and 5.3 refer to the impact of initial Ni(II) concentration and the pre-set time frames for the current system, at varying ranges. Graphical representations (Figures 5.7& 5.8), go hand in hand with the tabulated values, where a rapid sorption is recorded upto 10 minutes, after which a gradual decline is found. Also, maximum Ni(II) adsorption had occurred at 25 mg/L, thereby the aforesaid concentration and time interval have been chosen for rest of the experiments.

Table 5.2 Effect of Initial Concentration & Contact time [Ni(II)-TPVSP]

TPVSP	Percentage Removal (%)					
	5 mg/L	10 mg/L	15 mg/L	20 mg/L	25 mg/L	30 mg/L
5	33.67	43.67	68.13	75.54	88.08	70.81
10	42.32	52.47	66.78	89.70	96.54	89.25
15	31.88	69.52	72.83	88.14	90.35	72.65
20	23.45	39.09	63.92	74.91	77.68	68.51
25	25.73	43.03	56.67	69.33	78.80	59.41
30	27.40	29.40	38.81	40.70	79.61	55.67

Table 5.3 Effect of Initial Concentration & Contact time [Ni(II)-TBVSP]

TBVSP	Percentage Removal (%)					
	5 mg/L	10 mg/L	15 mg/L	20 mg/L	25 mg/L	30 mg/L
5	35.25	45.40	60.07	72.61	80.37	75.45
10	37.65	53.22	78.18	85.41	93.47	80.47
15	41.21	54.63	71.29	78.25	80.70	70.41
20	35.18	58.50	74.93	85.71	88.91	62.94
25	34.24	53.77	70.39	75.24	90.86	59.30
30	32.14	48.03	64.44	50.47	83.21	48.25

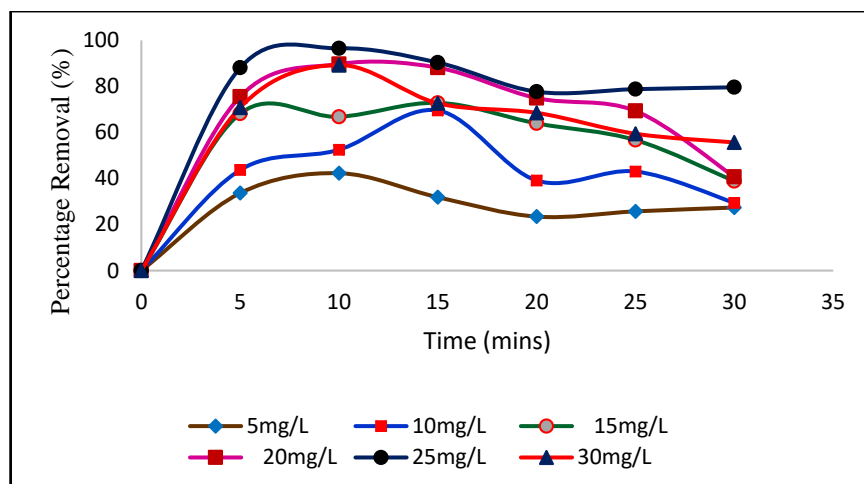


Figure 5.7 Effect of Initial Concentration & Contact time (TPVSP)

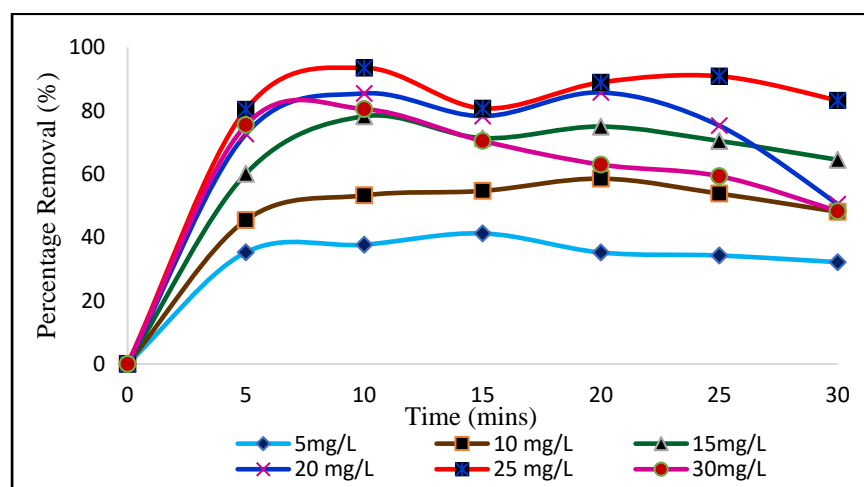


Figure 5.8 Effect of Initial Concentration & Contact time (TBVSP)

5.3.3 Effect of Dosage

The influence of adsorbent doses (10- 100 mg: 25 mg interval) are presented in tables 5.4 and 5.5 with corresponding curves in figures 5.9, 5.10. A maximum adsorption percentage registered for 100 mg, beyond which a decrease is noted. Saturation of active sites through the sorption reaction might have occurred².

Table 5.4 Effect of Dosage [Ni(II)-TPVSP]

Time (mins)	Percentage Removal (%)				
	10 mg	25 mg	50 mg	75 mg	100 mg
5	33.2	35.1	40.0	58.2	85.7
10	35.3	40.4	48.1	69.7	98.2
15	38.6	42.2	56.2	78.1	97.4
20	38.3	55.6	65.3	72.5	90.2
25	37.2	52.3	63.4	70.2	88.4
30	34.3	52.1	60.1	69.5	81.2

Table 5.5 Effect of Dosage [Ni(II)-TBVSP]

Time (mins)	Percentage Removal (%)				
	10 mg	25 mg	50 mg	75 mg	100 mg
5	19.7	25.9	35.0	60.2	80.2
10	25.7	30.8	45.1	69.9	98.4
15	35.7	44.3	52.4	79.1	97.5
20	47.1	50.7	55.9	69.0	91.7
25	38.7	42.5	43.2	71.2	84.8
30	30.5	42.1	40.0	65.0	80.2

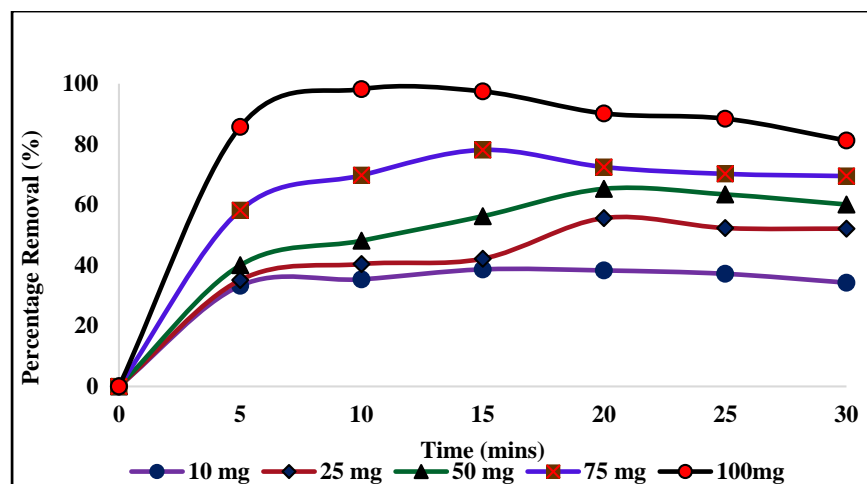


Figure 5.9 Effect of Dosage (TPVSP)

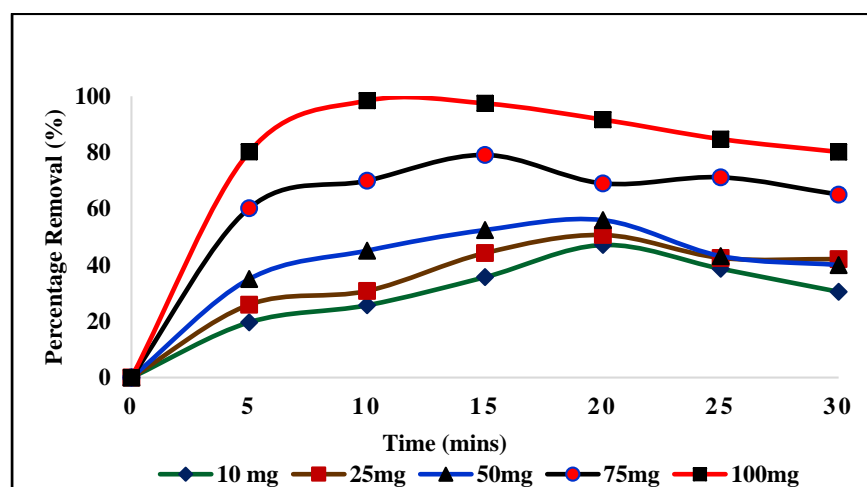


Figure 5.10 Effect of Dosage (TBVSP)

5.3.4 Effect of pH

pH 6.5 and pH 7 environs exhibited maximum Ni(II) sorption as evident from the inverted parabolas (Figures 5.11, 5.12). Preferential protonation and hydroxide precipitation may be the factors, responsible for decreased sorption at highly acidic and alkaline conditions³.

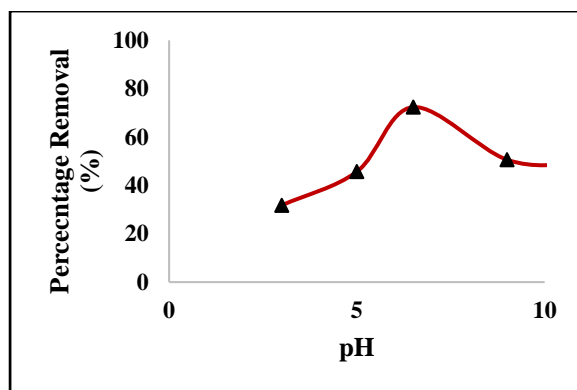


Figure 5.11 Effect of pH (TPVSP)

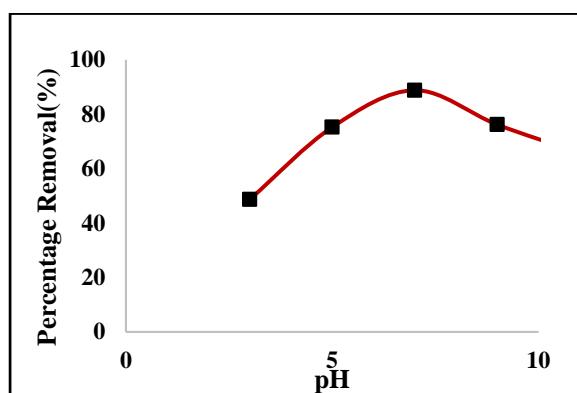


Figure 5.12 Effect of pH (TBVSP)

5.3.5 Effect of Cations/ Anions/ Co-ions

Table 5.6 Effect of Cations/ Anions/ Co-ions

Adsorbents	Percentage Removal (%)						
	Pb ²⁺ in the absence of ions	Cations		Anions		Co-ions	
		Na ⁺	K ⁺	Cl ⁻	SO ₄ ²⁻	Pb(II)	Cu(II)
TPVSP	93.0	89.1	85.2	91.3	92.4	90.2	92.3
TBVSP	96.2	92.5	90.6	94.1	95.3	93.7	94.2

Ionic influences over Ni(II)-TPVSP/ TBVSP systems, as listed in table 5.6 highlights notable inhibitions in Ni(II) removal in presence of K⁺ and Pb(II) ions. Whereas, minimal inhibition is registered by other ions even at higher concentrations which might be due to the inability of these ions to interfere the strong binding capacity between sorbate/sorbent species.

5.3.6 Effect of Temperature

Impact of temperature upon the studied systems at specified Kelvins (Table 5.7) supports the maximum Ni(II) sorption at 323 K. A comparatively greater Ni(II) removal at this increased temperature, may be due to the recurred mobility of ions to diffuse into their active sites⁴.

Table 5.7 Effect of Temperature

Adsorbents	Percentage Removal (%)			
	293K	303K	313K	323K
TPVSP	69.9	93.2	94.2	95.3
TBVSP	71.7	96.3	97.0	98.3

5.3.7 Desorption / Regeneration Studies

Varying strengths of HCl as eluent was employed to desorb the adsorbed Ni(II) species from the shell powders. The trend of desorption (Figure 5.13) is identical to that of Pb(II) system, wherein 0.1 N HCl registered a maximum desorption percentage, similar to the results as mentioned in chapter IV. TBVSP exhibited maximum retrieval efficiency in successive cycles in preference to TPVSP material.

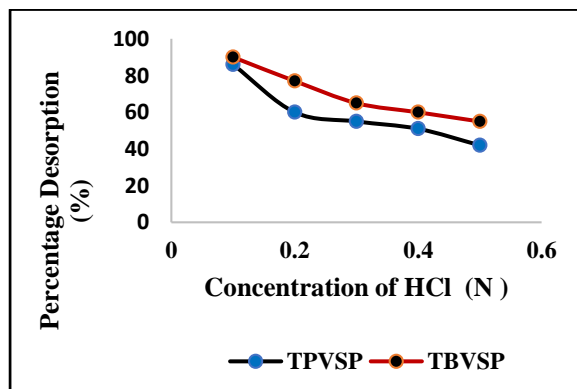


Figure 5.13 Desorption of Ni(II)

5.4 Isothermal Studies

The sorptive nature of adsorbents was verified using isotherm. Langmuir, Freundlich, and Dubinin-Kaganer-Radushkevich graphs were plotted with corresponding equilibrium concentrations (Table 5.8). Isothermal constants obtained from the respective slopes/ intercepts and separation factors (R_L) values are listed in tables 5.9 and 5.10

Table 5.8 Equilibrium Concentrations – Isothermal Data

Systems	Metal Ion Conc. (mg/L)	Langmuir		Freundlich		DKR	
		C_e	C_e/q_e	$\log C_e$	$\log q_e$	$\xi^2 \cdot 10^{-5}$	$\ln q_e$
Ni(II) - TPVSP	5	2.88	0.73	0.46	0.24	5.62	1.86
	10	4.75	1.81	0.68	0.62	2.31	1.96
	15	4.98	1.99	0.70	0.80	1.72	1.61
	20	2.06	0.23	0.31	0.28	9.94	2.29
	25	1.65	0.07	1.63	1.18	7.46	2.19
Ni(II) - TBVSP	5	2.34	0.38	0.37	0.12	8.04	2.86
	10	3.98	1.07	0.59	0.86	3.34	1.12
	15	3.27	0.66	0.51	0.77	4.51	1.77
	20	2.92	0.44	0.47	0.93	5.51	2.14
	25	1.83	0.14	0.21	0.07	4.49	2.46

Table 5.9 Isothermal Constants

Systems	Langmuir			Freundlich			DKR		
	q_m (mg/g)	b (L/g)	R^2	K_F (mg/g)	$1/n$	R^2	q_s (mg/g)	E (KJ/mol)	R^2
Ni(II) – TPVSP	2.31	0.62	0.9756	2.51	0.46	0.8987	1.11	1.25	0.6833
Ni(II) - TBVSP	1.72	0.66	0.9859	1.25	0.68	0.8157	5.25	2.76	0.8395

Table 5.10 Equilibrium Parameter (R_L)

Conc. (mg/L)	Pb(II)-TPVSP	Pb(II)-TBVSP
5	0.23	0.24
10	0.13	0.14
15	0.09	0.10
20	0.07	0.07
25	0.07	0.07
25	0.06	0.06

5.4.1. Langmuir Model

Langmuir plots of C_e/q_e vs C_e for Ni(II)-TPVSP/TBVSP systems are shown in figures 5.14 & 5.15 with respect to the initial concentrations. Sorption capacity ' q_m ' values as derived from the plots is comparable with experimental ' q_e ' values, favoring the systems. The linearity of the points, b and R_L values less than unity suffice the applicability of the model⁵.

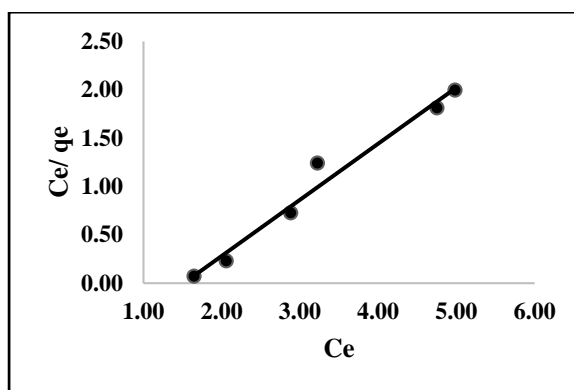


Figure 5.14 Langmuir Plot (TPVSP)

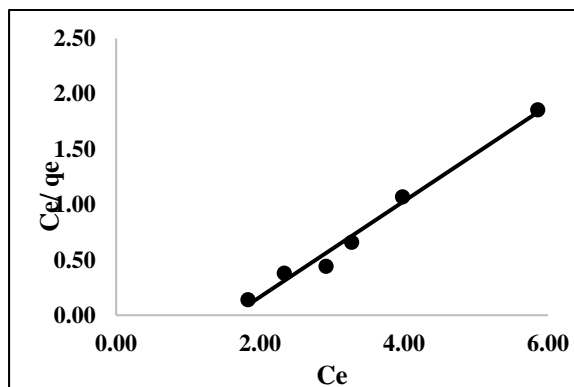


Figure 5.15 Langmuir Plot (TBVSP)

5.4.2 Freundlich Model

Figure 5.16 and 5.17 correspond to Freundlich model, where few points diverge away from the straight lines, even though $1/n$ values are less than unity ⁶, lower R^2 values are obvious than Langmuir. Thence, Freundlich model is less favored by the systems.

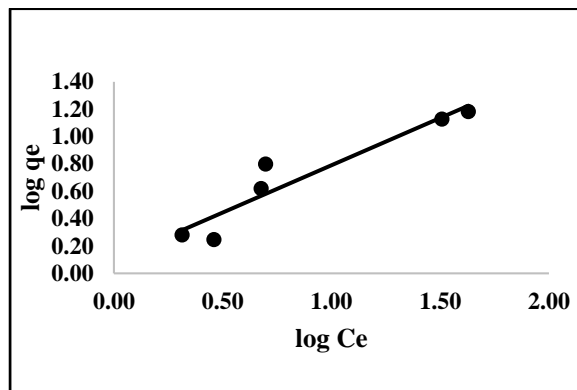


Figure 5.16 Freundlich Plot (TPVSP)

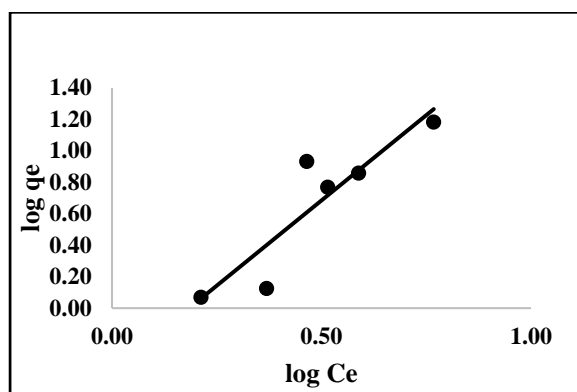


Figure 5.17 Freundlich Plot (TBVSP)

5.4.3 Dubinin–Kaganer-Radushkevich Model

Alike to the discussions done in the previous chapter, the sorbents' exhibited lower free energy values (< 8 KJ/mol) in support of physisorption mechanism⁷, which have been evidenced from the plot of $\ln q_e$ vs ε^2 (Figures 5.18 and 5.19).

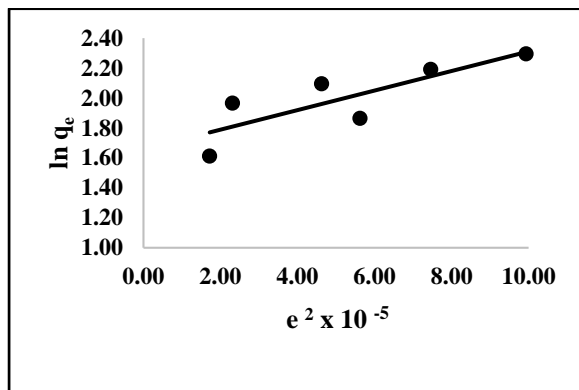


Figure 5.18 DKR Plot (TPVSP)

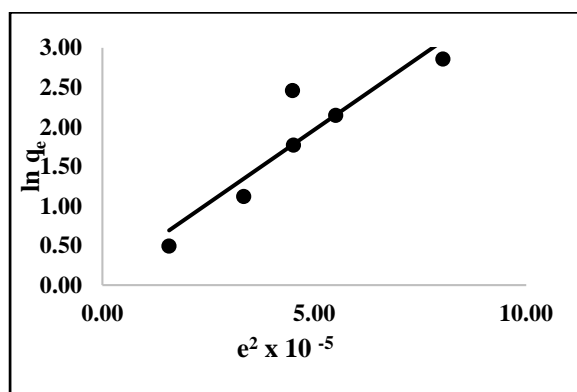


Figure 5.19 DKR Plot (TBVSP)

A judicious comparison made amongst the above discussed isothermal plots, reveal that both the systems obey the following order: Langmuir > Freundlich > DKR as observed in the previous chapter.

5.6 Adsorption Dynamics

ΔH° , ΔS° calculated from the slope and intercept of Van't Hoff 's plots (Figures 5.20 and 5.21) are presented in table 5.11. Nature of feasibility, spontaneity and endothermicity are arrived at from the negative values for ΔG° and positive values for ΔH° .

Positive ΔS° value shows the intensification of randomness at the sorption interface. The obtained results are in good agreement with that of N.M Andal et al.,⁸ in the removal of Cr(VI) using almond shell.

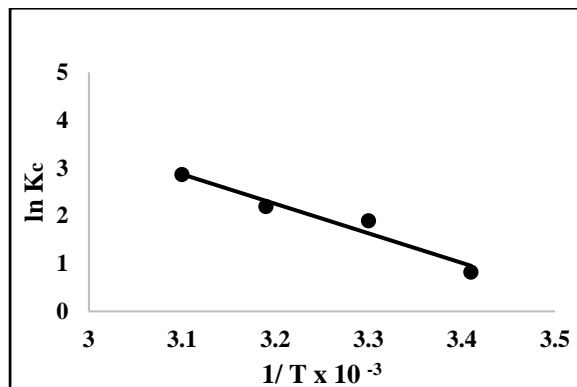


Figure 5.20 Van't Hoff's Plot (TPVSP)

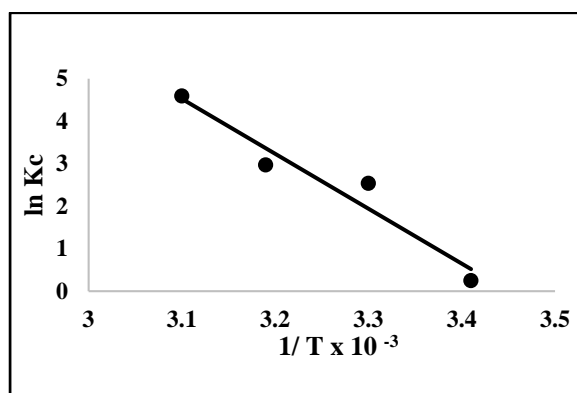


Figure 5.21 Van't Hoff's Plot (TBVSP)

Table 5.11 Thermodynamic Parameters

Temp. (K)	Ni(II) – TPVSP			Ni(II) – TBVSP		
	$\Delta G^\circ \times 10^{-3}$ (kJ/mol)	ΔH° (kJ/mol)	ΔS° (J/mol K)	$\Delta G^\circ \times 10^{-3}$ (kJ/mol)	ΔH° (kJ/mol)	ΔS° (J/mol K)
293	-0.04	6.17	22.01	-0.05	12.92	44.59
303	-0.64			-0.50		
313	-0.77			-0.55		
323	-0.96			-0.63		

5.7 Conclusion

Sequestration of Ni(II) ions is dealt in chapter V employing chemically modified shells of *Pistachio vera* and *bivalve* molluscs (TPVSP/TBVSP). The collected shells were crushed, sieved into different mesh sizes in prior to treatment. Sorption characteristics of the bare and their Ni(II) laden materials were investigated using microscopic, EDAX, SEM and FTIR studies. Adsorption of Ni(II) ions onto the sorbents was examined to optimize their excellent conditions through pilot batch studies and quantifications of the data was ensured through column trials. The operating parameters exhibited best results at 0.18 mm, 100 mg, 25mg/L and pH 6.5/ pH 7. Interference of other cations, anions and co-ions recorded negligible sorption inhibition in Ni(II) uptake by sorbents, thereby favoring their sorption potential. Reproducibility of exhausted materials were confirmed through proper desorption/ regeneration studies, where appreciable was encountered in the successive cycles. Isothermal and thermodynamic parameters were incorporated to access the nature of sorption process, thereby linear fit of Langmuir model favored monolayer sorption. Positive variation in enthalpy and entropy values and negative values for free energy charge reflected in the spontaneity, endothermicity and disorderliness of the reactions. Amongst TPVSP and TBVSP, the latter exhibited better Ni(II) removal efficiency (98%) rather than its former (90%). Thence, it is evident from the results that, TBVSP holds better sorption capacity in trapping heavy metal ions.

5.7 References

1. M.Yasmin Regina , S. Saraswathy , B.Kamal , V.Karthik , K. Muthukumaran, Removal of Nickel (II) Ions from Waste Water using Low Cost Adsorbents: A Review, *Journal of Chemical and Pharmaceutical Sciences*, 8 (1),(2015)
2. Najua Delaila Tumin, A. Luqman Chuah ,Z. Zawani , Suraya Abdul Rashid, Adsorption of Copper From aqueous solution by Elais Guineensis Kernel Activated Carbon, *Journal of Engineering Science and Technology*, 3(2), (2008)180 – 189
3. N. T. Abdel-Ghani, M. Hefny, G. A. F. El-Chaghaby, Removal of lead from aqueous solution using low cost abundantly available adsorbents, *Int. J. Environ. Sci. Tech.*, 4 (1) (2007) 67-73,
4. V.K. Gupta, A. Rastogi, Sorption and Desorption Studies of chromium(VI) from nonviable Cyanobacterium *Nostocmuscorum* Biomass, *Journal of Hazardous Materials*, 154, (2008) 347-354,
5. Shruthi K M ,Pavithra M P, A Study on utilization of Groundnut Shell as Biosorbent for Heavy Metals removal, *International Journal of Engineering and Techniques –* 4(3), (2018)
6. Mohammad Ghazi et al., Freundlich Isotherm Equilibrium Equations in Determining Effectiveness a Low Cost Absorbent to Heavy Metal Removal In Wastewater (Leachate) At Teluk Kitang Landfill, Pengkalan Chepa, Kelantan, Malaysia, *Journal of Geography and Earth Science* 1(1) (2013) 01-08
7. Daniel C. Emeniru, Okechukwu D. Onukwuli, Pere-ere DouyeWodu, Bernard I. Okoro, The Equilibrium and Thermodynamics of Methylene Blue Uptake onto Ekowe Clay; Influence of Acid Activation and Calcination, *International Journal of Engineering and Applied Sciences (IJEAS)*, 2(5) (2015)
8. N.Muthulakshmi Andal and G.Gohulavani, Sorption kinetics and equilibrium studies on the removal of toxic Cr(VI) ions employing modified Indian almond nut shells, *Journal of Energy Technologies and Policy*, 3(11) (2013).